

SIIV - 5th International Congress - Sustainability of Road Infrastructures

Pavement Pumping Prediction using Ground Penetrating Radar

Tosti F.^{a,*}, Benedetto A.^a

^a *Department of Sciences of Civil Engineering, University of Roma Tre, Via Vito Volterra 60, Rome 00146, Italy*

Abstract

In this paper we propose a novel inspection method based on Ground Penetrating Radar techniques to predict pumping and reduce the risk on safety. Experimental layouts are developed to measure the clay content in sub-grade/sub-base compacted soils. Typical road material is analyzed using two different GPR systems: three types of soils are adequately compacted in electrically and hydraulically isolated boxes. Bentonite clay is gradually added from 2% to 25% by weight. Signals are analyzed in both time and frequency domains, and the reliability of results is respectively validated by the electromagnetic and the Rayleigh scattering theory showing promising correlations.

© 2012 The Authors. Published by Elsevier Ltd. Selection and/or peer-review under responsibility of SIIV2012 Scientific Committee. Open access under [CC BY-NC-ND license](https://creativecommons.org/licenses/by-nc-nd/4.0/).

Keywords: pavement pumping; Ground Penetrating Radar; clay; electromagnetic theory; Rayleigh scattering theory

* Corresponding author. Tel:+39-06-57333261; fax: +39-06-57333441.
E-mail address: fabio.tosti@uniroma3.it

1. Introduction

Pavement structural damages are often revealed by the occurrence of pavement cracks, deformations, ruts or other fails. The sub-base is often affected by damage from the bottom with the structural failure in propagation to the top. The resulting cracking of the pavement produces unsafe driving conditions causing increase of the cost of rehabilitation and decrease of the efficiency of repair. It is difficult to identify the cause of a visible damage, as it can result from several different causes. If the detection of the cause is not correct, any rehabilitation could have only a short time period of effectiveness since only the symptoms are treated. The type of damage investigated in this paper is a structural damage, due to water and plastic soil infiltration in sub-asphalt layers. This kind of damage is classified in pavement engineering as pumping, and it is frequent in pavement designed on clay soils or on soils with clay fractions. Water infiltration and transport of clayey soil deeply affects the decrease of bearing capacity of the unbound layers [1-4].

Road bearing courses have to be characterized by very good mechanical properties to bear the heavy cycles of repeated loads. Although dry and wet conditions should not affect the bearing capacity of unbound layers, it is frequent that clay or fine soil fractions are transported by water in the unbound layers, causing a high risk of plastic deformation under repeated cycles of set loads.

Several causes originate pavement pumping. These may include inadequate compaction during construction or poor mix design, high water table and poor drainage. By project analysis, it is important to monitor the risk of pumping, checking the clay fractions of sub-grades and identifying the water table location [5]. In terms of pavement maintenance, fog seals or slurry seals may be applied to limit water infiltration in order to preserve pavement condition, safety and ride quality. Conversely, when a wide corruption affects the road structure, a structural and functional enhancement of a pavement is needed. The reduction of water movement can be obtained by improving sub-grade drainage. Alobaidi and Hoare [6] carried out small-scale laboratory tests for the development of a geo-composite for preventing and minimizing pumping of fines at the cohesive sub-grade sub-base/ ballast interface of a highway/railway pavement. Through an empirical heuristic approach, it was found that an anti-pumping geo-composite should have a high compression modulus, a low rebound under cyclic loading, a high in plane extensibility, a high load distribution ability and a high resistance to water movement.

Concerning the increase of the efficiency and the effectiveness of the repair, it is important to prevent any irreversible damage caused by pumping. In order to evaluate a relationship between pumping and the permanent deformation of pavement, Alobaidi and Hoare [7] developed a laboratory test which enabled measurements at the interface of sub-grade and sub-base for highway pavements. The amount of pumping was found to be directly related to the cyclic deformation of the system. Subsequently, similar tests were carried out to measure the pore water pressure at the interface between the sub-grade and sub-base/ballast layers causing the migration of fines from a subgrade soil into the overlying granular layer. The distribution under the contact area of a single sub-base particle with the sub-grade soil was investigated and thus the hydraulic gradients under different conditions of interface [8]. Ground Penetrating Radar (GPR) techniques are used to monitor non-destructively the moisture content in sub-asphalt soils with time-efficient and cost-effective procedures. GPR is based on the transmitting/receiving of an electromagnetic signal characterized by a given frequency. The most commonly measured electromagnetic properties is the dielectric constant (ϵ_r). Assuming that the porous media is a mixture of three phases (solid, water and air), and since the dielectric permittivity of water is significantly different than that of air and solid materials, the dielectric constant of the mixture has a high reliance on the moisture content.

Many studies have been carried out concerning the relationship between the dielectric constant of a soil and its volumetric water content. Various empirical correlations have been proposed. Topp et al. [9] suggested one of the most common used expression, which is supposed valid for any mineral soil material. Another theoretical approach that relates the soil water content to the soil permittivity is based on dielectric mixing. The method uses the volume fractions and the dielectric permittivity of each soil constituent to derive an approximate correlation, using a self-consistent approximation that represents the medium with the multi-indicator mode [10].

Benedetto and Pensa [11] proposed to evaluate the hydraulic permittivity fields in sub-asphalt structural layers and soils from the moisture maps observed with GPR. This method can be used to diagnose the presence of clay or cohesive soil that compromises the bearing capacity of sub-base and induces pumping damage. In some cases, the dielectric permittivity is estimated from the amplitudes of the transmitted and reflected signals [2]. In any case, the described methods require preventive calibration to estimate the signal velocity of propagation.

A more efficient and self-consistent approach is based on the GPR processing in the frequency domain. Lambot et al. [12,13] investigated the subsurface electric characteristics considering the dependence between the imaginary part of the dielectric permittivity and the frequency. Recent studies are based on Rayleigh scattering according to the Fresnel theory. The scattering produces a non-linear frequency modulation of the electromagnetic signal, where the modulation is a function of the water content. The laboratory tests have provided five different types of soil gradually wetted in under controlled conditions and analyzed using GPR. A high correlation between the shift of the frequency spectrum of the radar signal and the moisture content was demonstrated. The technique has also shown the potential for detecting clay content in soils and prevent pavement pumping damages [14].

Nomenclature

$h(t)$	transmitted signal
$y(t)$	received signal
I	total amount of replicas
$h_i(t)$	i-th replicas with different amplitudes
$\{a_{ij}\}_{i=1,I}$	amplitudes
$\{\tau_i\}_{i=1,I}$	delays
$e(t)$	random noise
E	$Re [E_0 e^{j\omega t}]$ [V/m]
E_0	electric field intensity [V/m]
ω	wave frequency [rad/s]
z	vertical value along the propagation direction [m]
μ	magnetic permeability [H/m]
$\varepsilon = \varepsilon' - j\varepsilon''$	permittivity or dielectric constant [F/m] as difference between the real and the imaginary part
$\sigma = \sigma' + j\sigma''$	electric conductivity [ohm/m]
$\varepsilon_0 = 8.854 \cdot 10^{-12}$	permittivity of free space [F/m]
$\varepsilon_r' = \varepsilon'/E$	real part of the relative permittivity
$\varepsilon_r'' = \varepsilon''/\varepsilon_0$	imaginary part of the relative permittivity
c	propagation velocity in free space [3×10^8 km/s]
v	propagation velocity in the medium
ε_r	dielectric constant (or relative permittivity) of the soil sample
A_l	amplitude of the reflection from the surface [V]
A_m	amplitude of the reflection from large metal plate [V]

r	thickness of the soil sample
Δt	time delay of the signal
ω	moisture content [%]
f_p	frequency peak value [Hz]
A, B	regression coefficients

2. Objective

The main objective of the work is the development of a novel inspection method based on GPR technique to predict the presence of clay in pavement structural layers under dry conditions and prevent damages due to pavement pumping. Data are post-processed in the frequency domain, according to the Rayleigh scattering method based on the Fresnel theory. The method has been tested in sub-grade and sub-base soils using different GPR systems to evaluate as it performs. This new technique can be supported by other survey methods, improving the quality of the results.

3. Theoretical background

3.1. The electromagnetic theory

GPR analysis is a geophysical technique in which an electromagnetic (EM) impulse is transmitted in the soil and the reflections are then collected through an antenna(s).

Analytically, the received signal $y(t)$ can be represented in time domain as the sum of multiple scaled and delayed replicas of the transmitted pulse signal plus noise. The considered model follows the general equation [15]:

$$y(t) = \sum_{i=1}^I a_i h(t - \tau_i) + e(t) \quad (1)$$

The EM plane wave propagation in a homogeneous medium is described by the Maxwell equation:

$$\frac{\partial^2 E}{\partial z^2} = -\omega^2 \mu \varepsilon E \quad (2)$$

The solution of Equation (2) is:

$$E = E_0 e^{-jkz} \quad (3)$$

with the propagation constant k given by:

$$k = \omega \sqrt{\mu \varepsilon (1 - j \tan \delta)} \quad (4)$$

where:

$$\tan \delta = \frac{\frac{\sigma}{\varepsilon_0} + \omega \varepsilon_r''}{\omega \varepsilon_r'} \quad (5)$$

is the loss tangent.

Considering $\omega \gg \sigma'$ and $\omega \gg \sigma''$ and $\varepsilon'' \ll \varepsilon'$, it is possible to write the following approximation:

$$v = \frac{c}{\sqrt{\frac{\varepsilon'}{\varepsilon_0}}} = \frac{c}{\sqrt{\varepsilon_r'}} \quad (6)$$

Thus, v is dependent on the dielectric properties of the surveyed medium, varying on the type of material. Regarding the pavement engineering, the unbound layers are unsaturated porous media, characterized by a mixture of three phases (solid, water and air). The dielectric constants of these materials are deeply different: air has a dielectric constant of 1, aggregate from 3 to 8 and water 81. Thus, the dielectric constant of the mixture is highly sensitive to water content.

Moreover, by monitoring the amplitudes and time delays between peaks, it is possible to evaluate both layer dielectrics and thicknesses [16]. The main equations are summarized below:

$$\varepsilon_r = \left(\frac{1 + A_1 / A_m}{1 - A_1 / A_m} \right)^2 \quad (7)$$

$$r = \frac{v\Delta t}{2} \quad (8)$$

3.2. Rayleigh scattering method

The main advantage of this method is that it does not require any field calibration. The signal is processed in the frequency domain; this method is based on Rayleigh scattering according to the Fresnel theory [14]. The scattering produces a non-linear frequency modulation of the electromagnetic signal, where the modulation is dependent on the water content. The moisture content is predicted by the following regression law:

$$\omega = (A - f_p) / B \quad (9)$$

A and B are calibrated with experimental data coming from laboratory tests and carried out on different types of soil. The value of the peak of frequency is extracted from the frequency spectrum of the reflected radar signal calculating the Fast Fourier Transform. The values of A range from 5.3×10^8 to 7.0×10^8 and the values of B from 1.1×10^7 to 2.3×10^7 , in function of the investigated type of soil [14].

4. Experimental analysis

4.1. Experimental design

The experimental design is focused on the evaluation of clay content in unpaved soils under dry condition. For these purposes typical road materials used for sub-base and sub-grade construction are employed. Clay is gradually added to simulate different levels of pumping. Protocol procedures has been preliminarily carried out in order to provide adequate mixing and compaction characteristics for the tested soils.

As regard to the mixing protocol, some iron filings of known weight has been mixed to a sandy soil at different time steps and subsequently sampled, in order to evaluate the uniformity of the mixing. It has been found that for a starting clay percentage of 2% by weight, the added material is uniformly distributed.

A vibration table has been used to compact the tested soil at different time steps. The corresponding measures of density have been compared to the values arising from Standard Proctor tests [17]. Results indicate that 60 seconds of vibration allows to obtain the same density as the modified Proctor with the large mold.

For cross checking, the bulk density of each soil sample is evaluated.

4.2. Tools and equipment

Different GPR systems are used to carry out the analysis. Figure 1a shows the multi-channel radar used with ground-coupled antennae (RIS/MF system manufactured by IDS S.p.A., Italy). The GPR uses two antennae with

central frequencies of 600 and 1600 MHz. The GPR measurements are developed using 4 channels: 2 mono-static and 2 bi-static. The received signal is measured in the time domain every $dt=7.8125 \times 10^{-2}$ ns. Only the signals of the mono-static channel 600×600 MHz are post-processed. The mono-static signal at 1600 MHz and the two bi-static signals are used for cross checking. The GPR is placed over the samples located in a box 0.40×0.40 m and 0.13 m high, so that the tested sample of soil is 0.33×0.33 m and 0.10 m thick. The box is idraulically and electrically isolated. The bottom of the box is on a metal plate in order to obtain a total reflection.

Another radar (Figure 1b) is used with ground-coupled antennae in a bi-static configuration and common offset; the transmitter and receiver are linked by optic fiber electronic modules and operate at 500 MHz central frequency (pulseEKKO PRO manufactured by Sensors and Software Inc., Canada). The received signal is sampled in the time domain at time steps of 7.8125×10^{-2} ns.

A Vector Network Analyzer (VNA) acquires ultra-wide band data in a bandwidth from 500 MHz to 3000 MHz. The signal is sampled in the frequency domain with approximately 1.56 MHz frequency steps. A double-ridged broadband horn antenna is connected via a high-quality coaxial cable to the VNA pulse generator and illuminates the analyzed target in a mono-static off-ground configuration (Figure 1c).

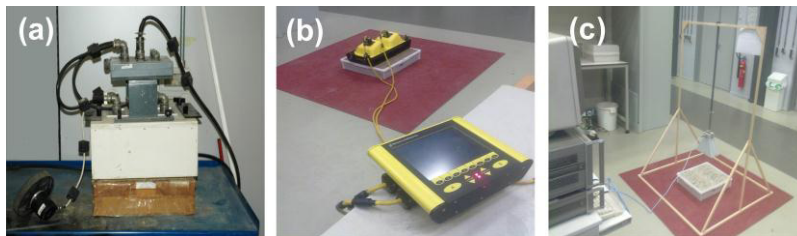


Fig. 1. GPR systems used for the analysis. (a) 600-1600 MHz ground-coupled radar; (b) 500 MHz ground-coupled radar; (c) Vector Network Analyzer

The soil samples are located in a box 0.45x0.55 m and 0.12 m deep, so that their reference dimension is 0.47x0.40 m and 0.10 m thick. The backscattered signal is totally reflected by a large metal plate at the bottom of the box. In all cases antennae positions and boxes dimensions and materials make negligible any edge effects within the range of the tested thickness. Moreover, all the GPR systems are calibrated in standard conditions (Laboratory temperature $19 \text{ }^\circ\text{C} \pm 2.5 \text{ }^\circ\text{C}$; relative humidity $45\% \pm 15\%$; absolute pressure about 1 atmosphere).

4.3. Materials and laboratory tests

Road materials typically employed for sub-grades and sub-bases construction are used. The so called Misto della Magliana alluvial soil (grain size 0-5 mm, classified as A1 by AASHTO) is tested with the 600-1600 MHz central frequency radar. Clay is gradually added from 2% to 30% by weight in steps of 2% and uniformly mixed (Figure 2). Totally, 16 tests are carried out. The mineralogy of the inspected clay is mainly montmorillonite. The particles are plate-shaped with an average diameter of approximately one micrometer. This mineral is a very soft phyllosilicate that forms in microscopic crystals.

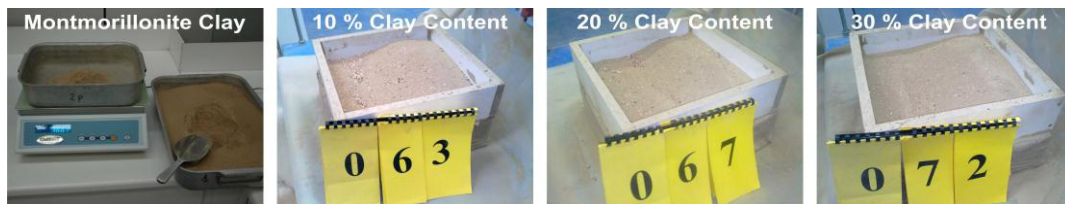


Fig. 2. Soil samples at different montmorillonite clay content (A1 Misto della Magliana)

Moreover, three types of soils, classified as A1, A2, A3 by AASHTO are used and adequately compacted in electrically and hydraulically isolated boxes. Figures 3a, 3b and 3c show respectively gravel (grain size 4-8 mm) as A1, coarse sand (grain size 1-2 mm) as A2, and fine sand (grain size 0.125-0.250 mm) as A3 soil type. These soils are analyzed both with the 500 MHz central frequency ground-coupled radar, in contact with the soil surface, and the VNA. Clay arising from natural sodium bentonite (Figure 3d) is gradually added from 2% to 25% by weight in steps of 2% and 5%. In total 27 tests, equally divided for each of the three investigated soils, are developed.

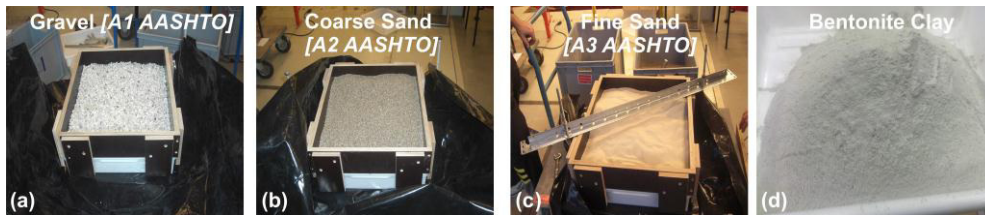


Fig. 3. Soil samples used for bentonite clay detection. (a) A1 gravel; (b) A2 coarse sand; (c) A3 fine sand; (d) bentonite clay

5. Results and short discussion

For each test the radar signal is post-processed. Low-pass and high-pass electronic filters are used to remove noise from the inspected radar signal. After filtering the signal, time domain analysis are carried out: results are focused on the dielectric permittivity of soils, the time delays between pulses reflections and the attenuation of the signal amplitude. As regard to the frequency domain analysis, fast Fourier transform (FFT) is employed to extract the frequency spectrum. The peak frequency of the spectrum f_p , which is the component of the signal with the largest amplitude, is measured for increasing clay content. Here the outcomes of the tests carried out using the 600-1600 MHz GPR and the A1 alluvial silty soil are presented and discussed. The outcomes of the other additional tests are currently in process and the first results confirm what is here discussed. In the next future, the work will be completed and widely presented.

4.4. GPR 600/1600 MHz test results and discussion

4.4.1. Density and plasticity characteristics of soil samples

The increasing amount of clay causes the intrusion of fine materials inside the air voids of the tested samples. Thus, it is expected a higher value of the soil sample density as the clay content increases. Moreover, the plasticity characteristics of the inspected soils are function of the clay content and its interaction with the mineralogy and texture of the tested sandy soil. In particular, for higher clay content, the measured Plasticity Index (PI) remains fairly constant. Figure 4 shows the density parameters registered for the soil samples.

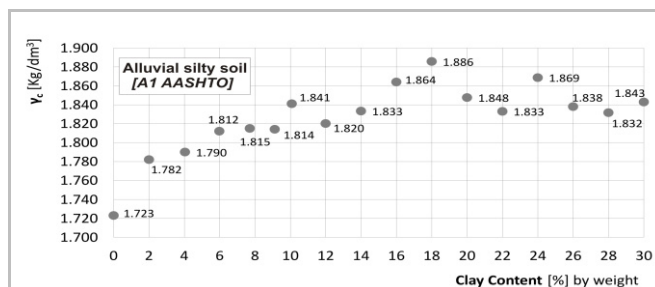


Fig. 4. Density vs. clay content in soil samples

4.4.2. Time Domain Analysis

According to Equation (1), the received signal is analyzed in time domain. Time delays Δt between pulses reflection are extracted to assess how the EM properties of soil samples are dissipative and affect the propagation velocity and the attenuation of GPR pulses in depth. Time delays between pulses reflection within single wavelets are analyzed to evaluate the signal attenuation. Moreover, time delays relating to the first and second pulses reflection are compared for all the tested soils to assess the influence of clay content on the wave propagation velocity in the medium (Figure 5).

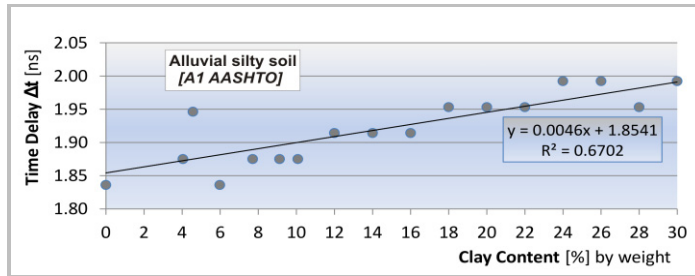


Fig. 5. Time delays between the first and second pulses reflection vs. clay content

In Figure 5, it is shown the increasing trend of time delays as the plasticity of soil increases. As expected, the wave propagation velocity in the medium decreases since the system is more dissipative: the intrusion of fine materials ($\epsilon_r = 7-9$) inside the air voids ($\epsilon_r = 1$) increases the value of the dielectric permittivity of the tested samples. Figure 6 shows the results for the expected rising trend of the dielectric permittivity ϵ_r .

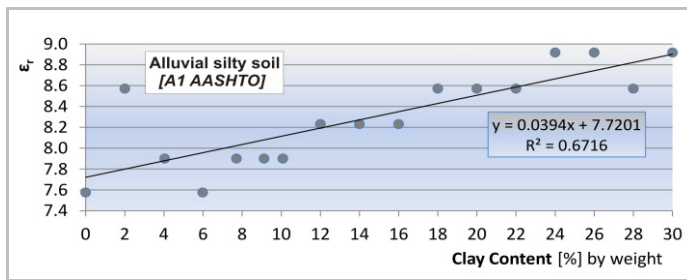


Fig. 6. Dielectric permittivity vs. clay content in soil samples

From Equation (6), as the dielectric permittivity ϵ_r increases, the wave propagation velocity v changes: greater time delays Δt are consequently registered (Equation 8). The results for amplitude attenuation analysis are given in Figure 7.

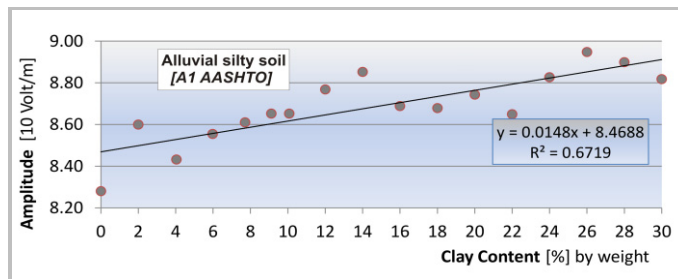


Fig. 7. Amplitude of pulses reflection vs. clay content in soil samples

As the clay content increases, the amplitudes of pulses reflection A of each soil sample decrease. This phenomenon can be related to a greater sensitivity of the signal toward the mineralogy of clay than the increasing of density values due to the intrusion of fine materials.

4.4.3. Frequency Domain Analysis

The frequency domain analysis demonstrates that frequency spectra shift not linearly (Figure 8a), as expected from the Rayleigh scattering theory based on the Fresnel theory. In fact, as the clay content increases, the hygroscopic water content increases causing a modulation of the spectra. Considering only the peak of the spectra, Figure 8b shows that the value of f_p weakly changes as the levels of clay content increase.

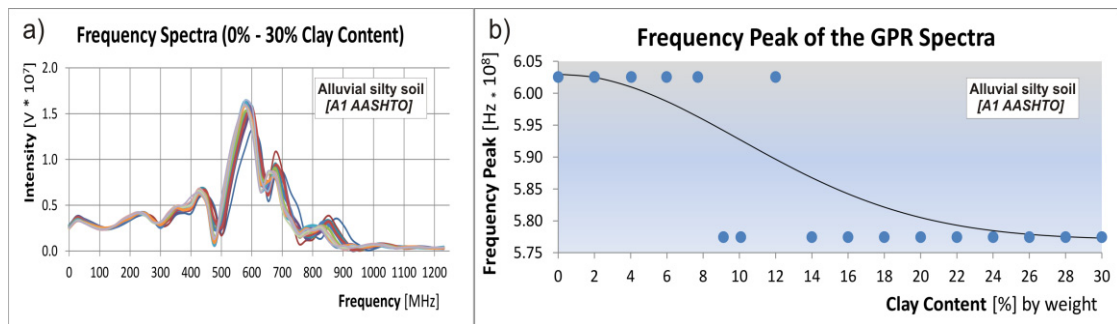


Fig. 8. (a) Frequency spectra modulation at different clay content; (b) Frequencies of spectrum peaks f_p for increasing levels of clay

This modulation depends on the water content (Equation 9) and, indirectly, on the clay content. The correlation between the central frequency values of the spectra and the clay content is negative: decreasing values of the central frequency correspond to increasing values of clay content, from 0% up to 30% by weight. This can be related to the clay hygroscopic capability involving a residual water content also in dry condition.

Moreover, comparative analysis of spectra have been done to evaluate a potential selective behavior of clay to specific frequency ranges (Figure 9).

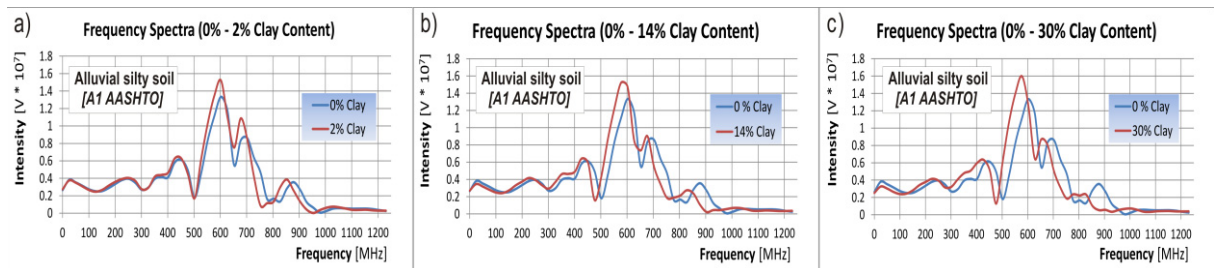


Fig. 9. Comparative analysis of frequency spectra. (a) low level of clay content; (b) medium level of clay content; (c) high level of clay content

From Figures 9a, 9b and 9c it is evident that at lower frequencies (< 500 MHz) the shape of the spectra is maintained. At central frequencies (500-700 MHz), the modulation of the spectra determines increasing values of frequency peaks as the clay content increases. Conversely, at higher frequency ranges, from 700 MHz up to 1100 MHz, an attenuation of the shape of the spectra is observed. It reasonably means that the energy dispersion increases at high frequency, as it is theoretically expected: in fact, clay content increases and the dielectric constant is higher because of the hygroscopic water content increases.

Conclusions

In this study, a novel inspection method based on GPR technique is presented to predict pavement pumping. Laboratory tests are carried out on heterogeneous and plastic soils using GPR instruments with different configurations and central frequencies. The signals are analyzed in both time and frequency domains.

In the time domain, good level of correlation among the measured parameters are obtained. As expected from the EM theory, it is demonstrated that the intrusion of clay material affects the dielectric properties of the soil samples in terms of permittivity, wave propagation velocity and time delays between pulses reflections. Regarding the signal amplitudes, increasing values are registered for higher clay rates: these can be related to the mineralogy of clay, mostly affecting the signal absorption than the contribution of higher grades of compaction.

In the frequency domain, the results are highly consistent for all the investigated soils. Assuming a residual water content of the dry clay due to its hygroscopic capability, frequency spectra shift not linearly, as expected from the scattering theory. It is demonstrated that the shift of the peak frequency provides information on the moisture content of a soil sample, and, indirectly on its clay content. Moreover, some considerations are provided in terms of comparative analysis of spectra, evaluating the potentiality of a selective behavior of clay to specific frequency ranges. These promising results show that further research is needed to clearly define an operational procedure to accurately measure the presence of clay from the shift of the frequency spectrum.

References

- [1] Kelley, E.J. (1999). Soil moisture effects in pavement systems. M.S.thesis, Ohio University, Athens.
- [2] Al-Qadi, I.L., Lahouar, S., Loulizi, A., Elseifi, M.A., & Wilkes, J.A. (2004). Effective approach to improve pavement drainage layers. *Journal of Transportation Engineering*, 130 (5), 658–664.
- [3] Zuo, G., Drumm, E.C., Meier, R.W., Rainwater, N.R., Marshall, C., & Wright, W.C. (2004). Observed long-term water content changes in flexible pavements in a moderate climate. *Proceedings of Geo-Trans Geotechnical Engineering for Transportation Projects*. Los Angeles, California, USA, 1 (126), 10 pp.
- [4] Diefenderfer, B.K., Galal, K., & Mokarem, D.W. (2005). Effect of subsurface drainage on the structural capacity of flexible pavement. VTRC 05-R35. Project, USA, 66818, 29 pp.
- [5] Washington State Department of Transportation (2012). WSDOT Pavement Guide, Interactive guide from WSDOT, USA.
- [6] Alobaidi, I. & Hoare, D. (1998). Qualitative criteria for anti-pumping geocomposites. *Geotextiles and Geomembranes*, 13 (4), 221-245.
- [7] Alobaidi, I. & Hoare, D. (1994). Factors affecting the pumping of fines at the subgrade - subbase interface of highway pavements: a laboratory study. *Geosynthetics International*, 1 (2), 221-259.
- [8] Alobaidi, I. & Hoare, D. (1996). The development of pore water pressure at the subgrade - subbase interface of a highway pavement and its effect on pumping of fines. *Geotextiles and Geomembranes*, 12 (1), 111-135.
- [9] Topp, G.C., Davis, J.L. & Annan, A.P. (1980). Electromagnetic determination of soil water content: measurements in coaxial transmission lines. *Water Resources Research*, 16 (3), 574–582.
- [10] Fiori, A., Benedetto, A. & Romanelli, M. (2005). Application of the effective medium approximation for determining water contents through GPR in coarse-grained soil materials. *Geophysical Research Letters*, 32, L09404. doi:10.1029/2005GL022555.
- [11] Benedetto, A. & Pensa, S. (2007). Indirect diagnosis of pavement structural damages using surface GPR reflection techniques. *Journal of Applied Geophysics*, 62 (2), 107-123.
- [12] Lambot, S., Slob, E.C., van den Bosch, I., Stockbroeckx, B. & Vanclooster, M. (2004). Modeling of ground-penetrating radar for accurate characterization of subsurface electric properties. *IEEE Transactions on Geoscience and Remote Sensing*, 42 (11), 2555-2568.
- [13] Lambot, S., Weiermüller, L., Huisman, J.A., Vereecken, H., Vanclooster, M. & Slob, E.C. (2006). Analysis of air-launched ground-penetrating radar techniques to measure the soil surface water content. *Water Resources Research*, 42, W11403, pp. 12.
- [14] Benedetto, A. (2010). Water content evaluation in unsaturated soil using GPR signal analysis in the frequency domain. *Journal of Applied Geophysics*, 71 (1), 26-35.
- [15] Wu, R., Li, J. & Liu, Z.S. (1999). Super resolution time delay estimation via MODEWRELAX. *IEEE Transactions on Aerospace and Electronic Systems*, 35 (1), 294–307.
- [16] Maser, K.R., Scullion, T. & Briggs, R.C. (1991). Use of radar technology for pavement layer evaluation. Report of Texas Transportation Institute, USA.
- [17] American Society for Testing and Materials (2007). ASTM D698-07e1 Standard Test Methods for Laboratory Compaction Characteristics of Soil Using Standard Effort. Standard of ASTM, USA.